



ELSEVIER

---

---

surface science

---

---

Surface Science 348 (1996) 379–386

## Minimum energy 2D patterns of atoms adsorbed on a hexagonal lattice

Humberto Arce<sup>a,\*</sup>, W. Luis Mochán<sup>b,\*</sup>, J. Jesús Gutiérrez<sup>c</sup>

<sup>a</sup> Departamento de Física, Facultad de Ciencias, Universidad Nacional Autónoma de México, Apartado Postal 70-542, 04510 México, Distrito Federal, México

<sup>b</sup> Laboratorio de Cuernavaca, Instituto de Física, Universidad Nacional Autónoma de México, Apartado Postal 48-3, 62251 Cuernavaca, Morelos, México

<sup>c</sup> Departamento de Física, Facultad de Ciencias, Universidad Nacional Autónoma de México, Apartado Postal 70-542, 04510 México, Distrito Federal, México

Received 11 April 1995; accepted for publication 13 October 1995

---

### Abstract

We obtain the lowest energy 2D arrangements of atoms adsorbed on a hexagonal lattice, assuming rational coverage and a repulsive dipolar adsorbate–adsorbate interaction. To this end we exhaustively explore the ordered arrangements compatible with the coverage, including those that have multiatomic unit cells. For some coverages ( $\theta=1/3, 1/4$  and  $1/7$ ) we find a well defined ground state, and for others a nearly infinite degeneracy related to the possibility of creating dense arrays of linear defects with a negligible energy cost. We compare our results with some experimental determinations of surface structures in alkali overlayers on fcc (111) and hcp (0001) metal faces. Except for those systems that form islands, we have found agreement between our predicted ground states and experiment. Furthermore, no ordered structures with the coverages of our near degenerate states have been observed.

**Keywords:** Adatoms; Alkali metals; Atom–solid interactions, scattering, diffraction; Equilibrium thermodynamics and statistical mechanics; Platinum; Single crystal surfaces; Transition metals

---

### 1. Introduction

Alkali–metal adsorption has been studied for a long time [1], initially due to its importance for thermionic emission and later for its relevance in heterogeneous catalysis [2]. Although it is known that adsorption on those systems generally takes place at high coordination sites, it has been found that adsorption on fcc (111) and hcp (0001) might happen on the on-top sites. That behavior, which

was recently confirmed by several techniques [3–6], was first reported by Lindgren et al. for Cs on Cu(111) [7]. Later it was also found in K/Ni(111) [8] and for Rb [9] and K [10] over Al(111). In fact, the same substrate–adsorbate system might have different adsorption sites depending on the coverage [11]. For alkalis on Al(111), adsorption may turn into substitution under annealing without changing the adlayer periodicity [10,12–14]. It seems that the transition from on-top adsorption to substitutional sites is a collective effect involving the whole periodic adlayer [10]. Furthermore, island formation has

\* Corresponding author. Fax: +52 73 17 3077; E-mail: mochan@ce.ifisicam.unam.mx

also been observed [12] under appropriate conditions for alkali adsorption on Al(111), indicative of an effective attractive interaction [15].

Recently there has been pronounced interest in alkali adsorption on Al [12] and in Li adsorption on Be [16]. The interaction between the adsorbate's *s*-levels and the substrate's surface and bulk states has been found to yield a metallic attractive interaction between nearby adsorbates which leads to a condensation into islands [15] even at relatively low coverages  $\theta \approx 0.1$ . Furthermore, the low energy required to form a vacancy on an Al(111) surface and the screening of the dipolar adsorbate–adsorbate repulsion might favor the occupation of substitutional sites instead of the high coordination hole sites. These results were obtained by proposing a small set of adsorbate superstructures and performing total energy calculations at different positions employing the density-functional theory (DFT) scheme within the local density approximation [17].

However, there are many other systems such as alkalis adsorbed on transition metals [11,18–23], which exhibit a rich series of phases for different coverages with no indication of condensation into islands. For these systems, it is safe to assume a repulsive interaction which is necessarily of dipolar character at distances larger than the substrate's screening length [24]. The origin of this dipolar repulsion is the electronic charge rearrangement upon adsorption. To our knowledge, there are still no DFT calculations of the minimum energy configurations of alkali adsorption on transition metals due to the difficulties inherent in the treatment of the *d*-electrons. However, there are a few simplified calculations that take into account only the lateral interaction between adsorbates, and assume that the interaction with the substrate is so strong that adsorption is only possible at a discrete lattice of adsorption sites. For example, in Ref. [25] the optimum lateral arrangements for adsorption on fcc (111) and on hcp (0001) faces was studied assuming a hexagonal lattice of adsorption sites and employing a simple dipolar adsorbate–adsorbate interaction. By changing the latter lattice, this model has also been employed for adsorption on fcc (100) [25] and fcc (110) [26].

There are several questions which are not

addressed within this lattice-gas model, such as the nature of the adsorption sites and the energy of adsorption. However, it allows the study of the consequences of the competition between the adsorbate–adsorbate repulsion and the binding to the substrate. The former favors the formation of a triangular lattice which is incommensurate with the underlying lattice for some coverages, leading to frustration.

We have recently developed a simple scheme to find the lowest energy ordered arrangements for atoms adsorbed on any lattice. This scheme allows for multiatomic unit cells which had been neglected in previous work [25,27,28] and takes into account the long range of the dipolar interaction. It has been successfully applied to the study of adsorption on fcc (100) metals and where it led to an explanation for the absence of ordered phases at some rational coverages in the experimental results [29].

In this paper we apply our previously developed scheme to study the ground state ordered configurations of dipoles on an hexagonal lattice. In Section 2 we outline our method, and in Section 3 we present the results which are discussed and compared to those of previous research, and are employed to interpret experimental data on alkali adsorption on: fcc (111) and hcp (0001) transition metal surfaces. Finally, in Section 4 we present our conclusions.

## 2. Method

We consider atoms adsorbed in registry on a periodic substrate. We assume they interact among themselves through a repulsive concave potential, and that the ground state of the system is spatially periodic at rational coverage [30]. To find the minimum energy lateral arrangement we perform an exhaustive search among the possible periodic arrangements of the adsorbed overlayer. If the coverage is  $p/q$  we first build all possible parallelograms of area  $tq$  (in units of the area of the substrate's unit cell) that are in registry with the substrate, where  $t$  is a small integer, and we eliminate those cells that lead through tiling to duplicate Bravais lattices. Then we decorate each unit cell by locating an adsorbate at a vertex and specifying

in all possible ways the positions of the remaining  $tp-1$  adsorbates, and we proceed to calculate the adsorbate–adsorbate interaction energy of the lattice obtained by tiling the plane periodically with the decorated cell. By letting  $t$  take different values from a set of relative primes, this procedure accounts for the possibility of non-monatomic cells and therefore allows microscopic density fluctuations which have been neglected in previous works [25,27,28]. The analysis of these fluctuations in Ref. [29] led to an explanation for the absence of ordered phases at coverages  $1/6$  and  $1/7$  in the systems K/Ir(100) [31] and Cs/Rh(100) [32].

For the adsorbate–adsorbate interaction we consider only its dipolar contribution [33,34] which accounts for the charge rearrangement between adsorbates and substrate but is independent of its exact nature [12]. Therefore we take only two-body interactions, and we neglect screening and short-range corrections. We assume that for a given coverage the dipole moment is constant, although it might differ for different coverages. For efficiency reasons we truncate the potential at a convenient cutoff distance; to incorporate the infinite range nature of the dipolar interaction, we shift the pair potential to eliminate discontinuities at the truncation distance and we replace the residuals due to the truncation and to the shift with a continuous approximation. This procedure, detailed in Eq. (2) of Ref. [29], produces a continuous concave potential, eliminates spurious ground states as the interaction range is increased, and leads to a rapid convergence of the energy.

As a substrate we use an hexagonal lattice and assume that adsorption occurs at its vertices. This

model describes adsorption at fcc (111) and hcp (0001) on-top sites, but it describes equally well any of their two nonequivalent sublattices of hole sites.

### 3. Results and discussion

In Fig. 1 we show the lowest energy arrangements obtained for coverages  $\theta = 1/7$ ,  $1/4$  and  $1/3$ , which correspond to  $(\sqrt{7} \times \sqrt{7})R19.1^\circ$ ,  $(2 \times 2)$  and  $(\sqrt{3} \times \sqrt{3})R30^\circ$ , respectively. The results displayed in Fig. 1 agree with those calculated previously by Shinjo and Sasada [25], and have been observed experimentally [18]. Notice that the smallest distances from a given lattice site to its neighbors are given by  $d_1 = 1$ ,  $d_2 = \sqrt{3}$ ,  $d_3 = 2$  and  $d_4 = \sqrt{7}$ . Therefore, only for coverages  $\theta = 1/d_n^2 = 1, 1/3, 1/4, 1/7, \dots$ , is an equilateral distribution of atoms possible while keeping registry with the hexagonal substrate. Not surprisingly, these are the most favorable arrangements, as shown in Fig. 1. For coverages which are not of the form  $\theta = 1/d_n^2$  there is frustration since there are no commensurate hexagonal superstructures, and therefore a conflict arises between the mutual repulsion of the adsorbates, which is minimized in an equilateral superstructure [25], and the bonding to the substrate's lattice of adsorption sites.

Fig. 2a shows the minimum energy ordering we found for  $\theta = 1/6$ . It also agrees with Ref. [25], although it has not been found experimentally. We remark that when we employ a cutoff ratio less than  $3\sqrt{3}$  lattice parameter, an infinite degeneracy of the ground state of the system occurs. The

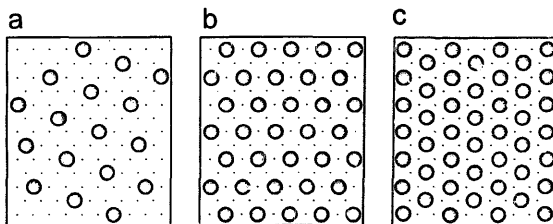


Fig. 1. Experimentally found patterns for K adsorbed on Pt(111) corresponding to the coverages  $\theta = 1/7$  (a),  $\theta = 1/4$  (b) and  $\theta = 1/3$  (c).

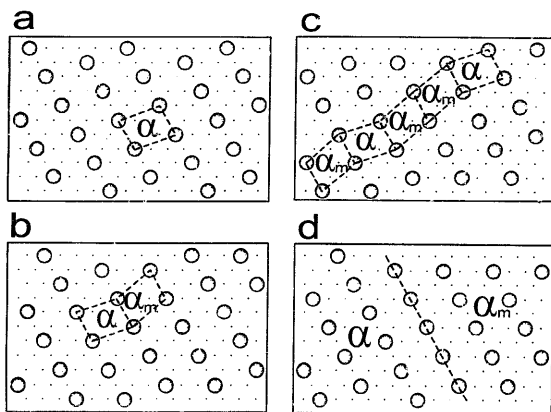


Fig. 2. Some of the lowest energy patterns for coverage  $\theta = 1/6$ . (a) Configuration with a monatomic primitive cell  $\alpha$ . The configuration in (b) has a diatomic cell made up of  $\alpha$  and a mirror image  $\alpha_m$ . (c) An arbitrary sequence of  $\alpha$  and  $\alpha_m$  cells, and (d) a twin boundary between a domain such as that in (a) and its mirror image.

different degenerate ground states may be built by joining the unit cells denoted by  $\alpha$  in Fig. 2b to their mirror images  $\alpha_m$ . This procedure yields orderings such as that in (b), where  $\alpha$  cells alternate with  $\alpha_m$  cells, that in (c), where we show an arbitrary sequence of  $\alpha$  and  $\alpha_m$  cells, and that in panel (d), where there is a segregation into two phases. Interestingly, even when we consider a very large interaction range of thousands of lattice parameters, the twin boundaries joining  $\alpha$  and  $\alpha_m$  regions cost a negligible amount of energy. A similar situation was found previously for adsorption on fcc (100) [29] and bcc (110) [26] with  $\theta = 1/6$ .

In Fig. 3 we illustrate the origin of the above situation. Solid dots indicate the occupied positions corresponding to the ground state shown in Fig. 2a, and some lines of adsorbates are labeled  $L_n$ ,  $n = 0, 1, 2, \dots$ . We have also introduced a stacking fault on the line  $L_0$  by displacing the atoms along the same line to their new position indicated by open dots. The interaction energy between the atoms of line  $L_0$  and those of line  $L_1$  is unchanged by the displacement, as can be easily confirmed by observing that for any solid dot A in line  $L_0$  there is

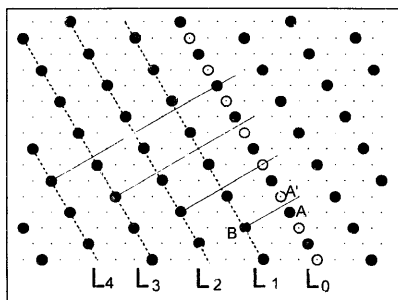


Fig. 3. Stacking fault within the  $\theta = 1/6$  configuration displayed in Fig. 2a. The original atomic positions atoms are represented by solid dots. The fault consists of a displacement of the atoms within the line labeled  $L_0$  to the positions indicated by open dots. We show neighboring atomic lines labeled  $L_n$ ,  $n = 1, 2, 3, 4$  and we draw a line from a typical atom B in  $L_1$  towards  $L_0$ . A and A' represent the adsorbate that is closest to this line before and after the displacement. Similar lines are drawn from  $L_2$ ,  $L_3$ , and  $L_4$ .

another open dot A' in  $L_0$  at the same distance from any adsorbate B in  $L_1$ , where A' is the image of A on a line through B perpendicular to  $L_0$ . The same argument shows that the stacking fault leaves the energy of line  $L_n$  unchanged, for any odd  $n$ . On the other hand if  $n=2m$  is even, the interaction energy changes by the amount

$$\frac{\Delta E_{2m}}{E_1} = (-1)^{1+m} \left( \frac{8}{(6m\sqrt{3})^3} + 2 \sum_{i=1}^{\infty} \frac{(-1)^i}{[(6m\sqrt{3}/2)^2 + i^2]^{3/2}} \right). \quad (1)$$

We obtain  $\Delta E_2/E_1 = 6.2 \times 10^{-8}$ , where  $E_1$  is the interaction energy among first neighbors. As a comparison we performed a similar calculation for  $\theta=1/7$ , the energy of a stacking fault in this case is six orders of magnitude larger, since in this case (Fig. 1a) there is no way of producing the fault without affecting the energies of the closest line of adsorbates. We conclude that for  $\theta=1/6$  even a

dense array of stacking faults, i.e. a larger unit cell such as that in Fig. 2c, costs a negligible amount of energy.

The  $\theta=1/5$  case is displayed in Fig. 4. The minimum energy ordering (a) differs from the monatomic lattice found by Shinjo and Sasada [25], and has not been observed. Similar to the  $\theta=1/7$  case on a square lattice [29], the minimum energy cell has a diatomic base; it may be constructed by joining unit cells of  $\theta=1/6$  and  $1/4$  ground states, which are indicated in Fig. 4a as  $\alpha$  and  $\omega$ . The  $1/5$  structure inherits from its  $\theta=1/6$  component the capability of supporting stacking faults of negligible energy. Thus, the orderings displayed in Figs. 4a and 4b are practically degenerate. This degeneration becomes exact if the interaction has a range smaller than  $4\sqrt{3}$  lattice parameters.

There is another kind of degeneration for the  $\theta=1/5$  ground state which becomes exact for a range less than  $2\sqrt{3}$  lattice parameters; an example of this is displayed in Fig. 4c. To explain this, in Fig. 4d we show the boundary between two segre-

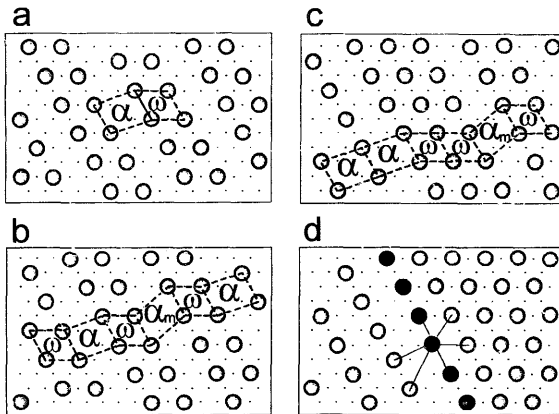


Fig. 4. Some of the lowest energy orderings for coverage  $\theta=1/5$ . (a) A configuration with a diatomic primitive cell made up by joining the primitive cell  $\alpha$  of the  $\theta=1/6$  ground state to the primitive cell  $\omega$  of the  $\theta=1/4$  ground state. The pattern in (b) has a primitive cell with four atoms within an area of 20. It is made by replacing every second  $\alpha$  cell in (a) by its mirror image  $\alpha_m$ . (c) An arbitrary sequence of  $\alpha$ ,  $\alpha_m$  and  $\omega$  cells yielding the same average coverage, and (d) a domain boundary between  $\theta=1/4$  and  $\theta=1/6$  monatomic phase. The distances from an atom in the interface to its first six neighbors are indicated.

gated domains, the first of which was generated by tiling a semiplane with unit  $\alpha$  cells, and the other by tiling with  $\omega$  cells. We indicate with solid dots those adsorbates lying on the boundary line, and with solid lines the distances to neighboring adsorbates up to  $2\sqrt{3}$  lattice parameters. Inspection of Fig. 4 shows that the distances  $d_5$ ,  $d_4$  and  $d_3$  appear one, one, and four times, respectively, for the adsorbates at the boundary, while they appear zero, zero and six times for an adsorbate within the  $\theta=1/4$  domain, and two, two and two times within the  $\theta=1/6$  domain. The boundary atoms contribute to the total energy the average between the contribution of an adsorbate within one region and another within the other zone. Therefore, the boundary costs no energy and any  $\theta=1/5$  configuration built by joining stripes of  $\alpha$  cells to stripes of  $\omega$  cells along their congruent sides will be degenerate for any possible choice of the individual stripe width. A similar phenomenon occurs in the square lattice with  $\theta=1/7$ .

Notice that our explanation for the near degeneracy of the  $1/5$  and  $1/6$  phases is based on geometric arguments, i.e. on the lowest distances that are modified by the introduction of a linear defect. Therefore, we expect that the phases displayed in Figs. 2a and 4a would have a near-infinite degeneracy, even if the potential were non-dipolar, as long as it is a distance-dependent pair-potential at large enough separation.

Various experiments have been made for low-temperature alkaline adsorption on the hexagonal faces (fcc (111) or hcp (0001)) of transition metals [11,18–23]. Experimentally, the general trend is as follows: (a) At low coverage diffraction rings are observed whose diameter depends on coverage. These patterns occur for coverages up to  $\theta \approx 0.12$ . (b) Between  $\theta \approx 0.12$  and  $0.25$  these rings coalesce into spots and these spots move and split until a  $(2 \times 2)$  pattern emerges. (c) If the adsorbate size is small enough a  $(\sqrt{3} \times \sqrt{3})R30^\circ$  superstructure appears after  $\theta=0.25$ . The transition between  $(2 \times 2)$  and  $(\sqrt{3} \times \sqrt{3})R30^\circ$  may occur in different ways in this coverage range.

Among the group of experiments referred to previously, the one made on K/Pt(111) at 120 K by Pirug and Bonzel [18] reports an additional

$(\sqrt{7} \times \sqrt{7})R19.1^\circ$  superstructure at  $\theta=1/7$ , besides the structures at  $1/3$  and  $1/4$  since K/Pt(111) seems to have a high thermal stability; the temperature at which the several phases reported become disordered is higher than for the other systems.

Comparing the results of our model with the experimental observations mentioned above, we find agreement with those superstructures reported at coverages  $1/7$ ,  $1/4$  and  $1/3$ . For coverage  $1/6$  we found a minimum energy arrangement that can have an infinite number of stacking faults with negligible energy costs. These stacking faults modify the orientation among near neighbors without changing the corresponding distances. After Ref. [35] we consider that they are associated with the ring diffraction pattern and the splitting in the diffraction points reported in Ref. [18] around this density. For coverage  $1/5$  we obtain a phase whose unit cell is diatomic but which also accepts an infinite number of linear defects with a small energy cost. Experimentally, no ordered phase with  $\theta=1/5$  has been reported. However, a  $(2 \times 2)$  hexagonal diffraction pattern corresponding to a  $(2 \times 2)$  phase has been observed in the whole range between  $\theta=1/5$  and  $1/4$  [18]. The diatomic unit cell we found for  $\theta=1/5$  contains both  $(2 \times 2)$  and  $(\sqrt{7} \times 3)R19.9^\circ$  cells. We have also explored the minimum energy orderings for several coverages within this interval ( $\theta=3/14$ ,  $2/9$ ,  $5/24$  and  $5/22$ ) and we display some of them in Fig. 5. We remark that they are constructed by a growing number of  $(2 \times 2)$   $\theta=1/4$  unit cells, their siblings rotated by  $\pm 120^\circ$  besides a few other  $\theta=1/4$  cells, and by  $(\sqrt{7} \times 3)R19.1^\circ$   $\theta=1/6$  cells  $\alpha$  and their mirror images  $\alpha_m$ . The  $(2 \times 2)$  cells organize themselves into hexagons, the proportion of which increases with coverage. It is important to note that from the phase diagram shown by Pirug and Bonzel the thermal stability of the  $(2 \times 2)$  pattern also increases with coverage.

#### 4. Conclusions

We have applied a recently developed simple method [29] to the study of adsorption of dipolar interacting atoms on a hexagonal lattice. The method consists of an exhaustive examination of

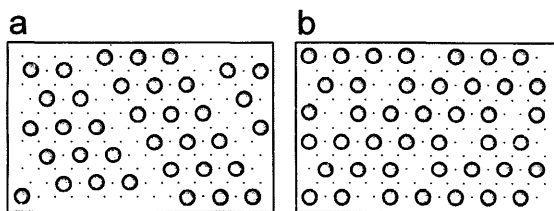


Fig. 5. Ground state patterns for selected coverages between  $\theta=1/5$  and  $\theta=1/4$ . (a) The lowest ordering for  $\theta=3/14$  which can be built by joining strips with  $\theta=1/6$  to strips with  $\theta=1/4$ . The structure in (b) corresponds to  $\theta=5/22$ . Note the organization of the  $\theta=1/4$  cells around hexagons.

all the possible arrangements of the interacting particles consistent with a given coverage and area of the primitive unit cell.

Clearly, our model could not attempt to explain systems for which the adsorbate–adsorbate interaction is not repulsive, the adsorption site is substitutional or there is island formation [12,16]. However, the charge rearrangement between the adsorbates and the substrate leads to a repulsive dipolar interaction at long distances, and therefore we expect our model to be adequate when the short-range interaction is also repulsive. We did not attempt absolute energy calculations; the energies we obtained were normalized to the energies of nearest-neighbor dipoles, and we ignored the binding energy. It is known that both of these change with coverage. Rather, we concentrated our attention on the relative energies of the different structures consistent with a given coverage.

Our results agree with the superstructures observed for several alkalis adsorbed on transition metals [11,18–23] for coverages  $\theta=1/3$  and  $1/4$ , and we also obtained the structure observed at  $\theta=1/7$  for K on Pt(111) at 120°K [18]. No superstructures with  $\theta=1/6$  and  $1/5$  have been reported. For coverage  $1/6$  we found that the optimum arrangement permits stacking faults with a negligible cost in energy, which yields an infinite number of nearly degenerated orderings with the same set of the next-neighbor distances, but with different orientations between them. The origin of this almost degeneracy is a geometrical characteristic of the arrangement at coverage  $1/6$  and further-

more, it is common to both square [29] and rectangular-centered [26] lattices. For  $\theta$  between  $1/5$  and  $1/4$  we found that the unit cells for the ground states are multiatomic, and can be built by joining the unit cells corresponding to  $\theta=1/6$  and  $1/4$ . This is possible since these unit cells have congruent sides. The ratio of  $1/4$  unit cells to  $1/6$  cells increases with coverage, such as the thermal stability of the  $(2 \times 2)$  diffraction pattern reported by Pirug and Bonzel [18].

In conclusion, our model, while using only dipolar interactions, leads to structures which are consistent with the experimental observations of ordered overlayers for only a few coverages  $\theta=1/3$ ,  $1/4$  and  $1/7$ . The model suggests an explanation for the absence of ordered phases with  $\theta=1/5$  and  $1/6$  given the infinite near-degeneracy of their calculated ground states. Furthermore, these structures are consistent with the observation of a  $(2 \times 2)$  diffraction pattern in the range  $\theta=1/5 \rightarrow 1/4$ , for which we obtained growing microdomains of a hexagonal  $\theta=1/4$  phase. We were able to understand the results above in terms of simple geometrical arguments, some of which remain valid even for non-dipolar potentials.

#### Acknowledgements

This work was partially supported by DGAPA-UNAM through grants No. IN-104594 and IN-104694. We thank Diana Davila for the technical support in the preparation of the manuscript.

## References

- [1] K.H. Kingdon and I. Langmuir, *Phys. Rev.* 21 (1923) 380.
- [2] H.P. Bonzel, *Surf. Sci. Rep.* 8 (1987) 43.
- [3] Z. Huang, L.Q. Wang, A.E. Schach von Wittenau, Z. Hussain and D.A. Shirley, *Phys. Rev. B* 47 (1993) 13626.
- [4] D.L. Adler, I.R. Collins, X. Liang, S.J. Murray, G.S. Leatherman, K.-D. Tsuei, E.E. Chaban, S. Chandavarkar, R. McGrath, R.D. Diehl and P.H. Citrin, *Phys. Rev. B* 48 (1993) 17445.
- [5] R. Davis, X.-M. Hu, D.P. Woodruff, K.-U. Weiss, R. Dippel, K.-M. Schindler, Ph. Hofmann, V. Fritzsche and A.M. Bradshaw, *Surf. Sci.* 307–309 (1994) 632.
- [6] A.V. de Carvalho, D.P. Woodruff and M. Kerkar, *Surf. Sci.* 320 (1994) 315.
- [7] S.A. Lindgren, L. Walldén, J. Rundgren, P. Westin and J. Neve, *Phys. Rev. B* 28 (1983) 6707.
- [8] D. Fisher, S. Chandavarkar, I.R. Collins, R.D. Diehl, P. Kaukasoina and M. Lindroos, *Phys. Rev. Lett.* 68 (1992) 2786.
- [9] M. Kerkar, D. Fisher, D.P. Woodruff, R.G. Jones, R.D. Diehl and B. Cowie, *Phys. Rev. Lett.* 68 (1992) 3204.
- [10] C. Stampf, M. Scheffler, H. Over, J. Burchhardt, M. Nielsen, D.L. Adams and W. Moritz, *Phys. Rev. Lett.* 69 (1992) 1532.
- [11] H. Over, H. Bludau, M. Skottke-Klein, G. Ertl, W. Moritz and C.T. Campbell *Phys. Rev. B* 45 (1992) 8638.
- [12] J.N. Andersen, E. Lundgren, R. Nyholm and M. Qvarford, *Surf. Sci.* 289 (1993) 307.
- [13] A. Schmalz, S. Aminpirooz, L. Becker, J. Haase, J. Neugebauer, M. Scheffler, D.R. Batchelor, D.L. Adams and E. Bøgh, *Phys. Rev. Lett.* 67 (1991) 2163.
- [14] J.N. Andersen, M. Qvarford, R. Nyholm, J.F. van Acker and E. Lundgren, *Phys. Rev. Lett.* 68 (1992) 94.
- [15] J. Neugebauer and M. Scheffler, *Phys. Rev. Lett.* 71 (1993) 577.
- [16] G.M. Watson, P.A. Brühwiler, H.J. Sagner, K.H. Frank and E.W. Plummer, *Phys. Rev. B* 50 (1994) 17678.
- [17] J. Neugebauer and M. Scheffler, *Phys. Rev. B* 46 (1992) 16067.
- [18] G. Pirug and H.P. Bonzel, *Surf. Sci.* 194 (1988) 159.
- [19] D.L. Doering and S. Semancik, *Surf. Sci.* 129 (1983) 177.
- [20] J. Hrbek, *Surf. Sci.* 164 (1985) 139.
- [21] W.C. Fan and A. Ignatiev, *J. Vac. Sci. Technol. A* 6 (1988) 735.
- [22] S. Chandavarkar and R.D. Diehl, *Phys. Rev. B* 38 (1988) 12112.
- [23] S. Chandavarkar, R.D. Diehl, A. Faké and J. Jupille, *Surf. Sci.* 211/212 (1989) 432.
- [24] A.G. Naumovets, in: *The Chemical Physics of Solid Surfaces*, Eds. D.A. King and D.P. Woodruff (Elsevier, Amsterdam, 1994) p. 167.
- [25] K. Shinjo and T. Sasada, *J. Phys. Soc. Jpn.* 54 (1985) 1469; *Dynamical Processes and Ordering on Solid Surfaces*, Eds. A. Yoshimori and M. Tsukada (Springer, Berlin, 1985) p.174.
- [26] L.D. Roelofs and D.L. Kriebel, *J. Phys. C Solid State Phys.* 20 (1987) 2937.
- [27] V.L. Pokrovsky and G.V. Uimin, *J. Phys. C* 11 (1978) 3535.
- [28] G. Cocho, R. Pérez-Pascual and J.L. Rius, *Europhys. Lett.* 2 (1986) 493.
- [29] H. Arce, W.L. Mochán and G. Cocho, *Surf. Sci.* 294 (1993) 108.
- [30] P. Bak and R. Bruinsma, *Phys. Rev. Lett.* 49 (1982) 249.
- [31] K. Heinz, H. Hertrich, L. Hammer and K. Müller, *Surf. Sci.* 152/153 (1985) 303.
- [32] G. Besold, Th. Schaffroth, K. Heiuz, G. Schmidt and K. Müller, *Surf. Sci.* 189/190 (1987) 252.
- [33] I. Langmuir, *J. Am. Chem. Soc.* 54 (1932) 2798.
- [34] J. Hölzl and L. Fritsche, *Surf. Sci.* 247 (1991) 226.
- [35] A.G. Naumovets, in: *The Chemical Physics of Solid Surfaces*, Eds. D.A. King and D.P. Woodruff (Elsevier, Amsterdam, 1994) p. 170.